A Consideration of Transient Response for Sensorless Model Control DC-DC Converter

Yudai Furukawa*, Shota Hirotaki*, Shingo Watanabe*, Fujio Kurokawa*, Nobumasa Matsui† and Ilhami Colak‡
*Graduate School of Engineering, Nagasaki University, Nagasaki, Japan
e-mail: fkurokaw@nagasaki-u.ac.jp
†Faculty of Engineering, Nagasaki Institute of Applied Science, Nagasaki, Japan
e-mail: MATSUI_Nobumasa@nias.ac.jp
‡Faculty of Engineering and Architecture, Gelisim University, Istanbul, Turkey
e-mail: icolak@gelisim.edu.tr

***Abstract*—The purpose of this paper is to discuss a current prediction algorithm for sensorless model control dc-dc converter. In the proposed method, the sensing resistor for the current detection is eliminated by predicting the output current. The output current is predicted from the equation of the relationship between the output and input voltage in the static state using the duty ratio and the output voltage. The predicted output current is substituted the static model. Two different equations according to the operation mode of the dc-dc converter are used for the current presumption. They should be switched smooth and seamless for the output current prediction.**

Keywords—*dc-dc converter*; *digital control*; *transient response*;

I. INTRODUCTION

The importance of energy saving has emphasized in accordance with the increase of traffic in the network society. The introduction of the high performance power management system is necessary [1]-[5]. Simultaneously, the reliability and the efficiency of the communication power supply must be high. In addition, the power supply is required the operation in the standby mode for the energy saving. Thus, it must return to the active mode quickly and its output voltage must be regulated from no load to full load. A digital control technology of the switching power supply has made remarkable progress in order to realize them. In the digital control, both the conversion time of A-D converter and the processing time of digital controller exert a bad influence on the transient characteristics. The improvement of the transient characteristics is important for the reliable telecommunications power supply.

The authors have already reported that the model control for the dc-dc converter is effective for the improvement of the static and transient characteristics. In the proposed method, not only the output voltage but also the output current and the input voltage are detected and used for the control calculation. Therefore, the bias value of the PID control is changed depending on the output current. The wide regulation range is realized in the heavy load from the light load. Also, the transient characteristics are improved without reducing the delay time. Although the existing proposed method achieves a superior transient response compared to the conventional PID control, the power loss occurs because the output current is detected using the sensing resistor.

This paper presents a current detection algorithm for sensorless model control dc-dc converter. In the proposed method, the sensing resistor for the current detection is eliminated by predicting the output current [6]-[8]. Although the output current is predicted from the equation of the relationship between the output and input voltage in the static state using the duty ratio and the output voltage, the switching of the equation is needed because two equations predicting output current exist corresponding to the operation mode of the dc-dc converter. The switching of the equation is based on properties of those equations. Hence, the output current is predicted properly and also the sensorless model control is achieved. Moreover, the fast transient response is realized compared with the conventional PID control.

II. OPERATION PRINCIPLE

Figure 1 shows a basic configuration of the main circuit. A main circuit is a buck type dc-dc converter. e_i is the input voltage, e_o is the output voltage, R is the load resistance and i_o is the output current. e_i and e_o are detected and converted into the digital value. These are sent to the digital control circuit. Then the on-time T_{on} is determined in the control circuit. The output current was detected in the existing model control. Thus, the sensing resistance was needed. However, the sensing resistance is eliminated in the propose method because the output current is predicted.

Figure 2 details the configuration of the digital control circuit. e_i and e_o are inputted into the pre-amplifier. They are amplified by A_{ei} and A_{eo} times, respectively. A_{ei} and A_{eo} are the gain of each pre-amplifier. These amplified voltages are inputted into the A-D converters and converted into the digital values $e_i[n]$ and $e_o[n]$

$$e_i[n] = G_{AD\_ei} A_{ei} e_i \quad (1)$$

$$e_o[n] = G_{AD\_eo} A_{eo} e_o \quad (2)$$

where G_{AD_ei} and G_{AD_eo} are the gain of the A-D converter for e_i and e_o. The index n denotes the sampling point obtained at the n-th switching period.

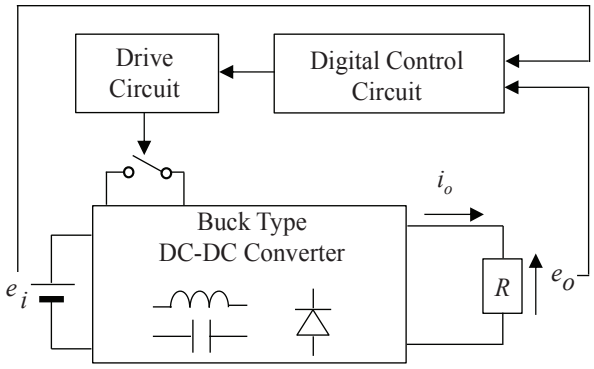

Fig. 1. Basic configuration of main circuit.

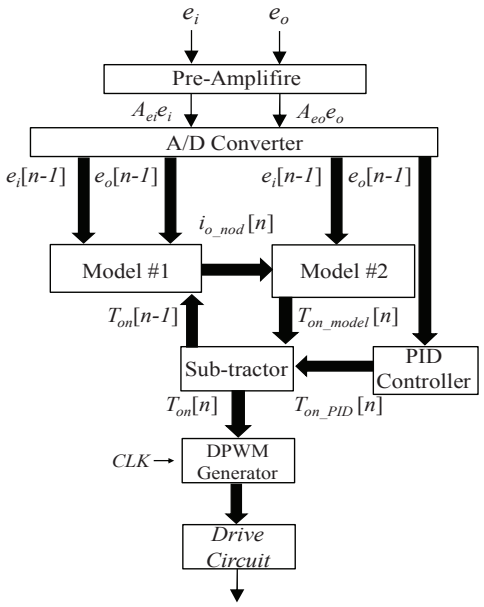

Fig. 2. Configuration of digital control circuit.

The digital control circuit consists of the output current prediction part (Model #1), the static model control (Model #2) and the PID control. $e_i[n\text{-}1]$ is sent to Model #1 and #2 and also $e_o[n\text{-}1]$ is sent to Model#1 and PID controller.

In Model #1, the predicted output current $i_{o\_nod}[n]$ is calculated by using the digital value $T_{on}[n\text{-}1]$ of on time, $e_i[n\text{-}1]$ and $e_o[n\text{-}1]$. The equation for the prediction of output current is explained in the next section.

The bias value $T_{on\_model}[n]$ is calculated in Model #2 by using $i_{o\_nod}[n]$ and $e_i[n]$. There are two equations for the calculation of $T_{on\_model}[n]$. They are expressed as follows:

$$T_{on\_model\_CCM}[n] = \frac{N_{Ts}}{(\frac{e_i[n]}{a} + V_D)}\left(E_o^* + r i_{o\_nod}[n] + V_D\right) \tag{3}$$

$$T_{on\_model\_DCM}[n] = N_{Ts}\sqrt{\frac{2Li_{o\_nod}[n](E_o^* + V_D)}{(\frac{e_i[n]}{a} + V_D)(\frac{e_i[n]}{a} - E_o^*)T_s}} \tag{4}$$

In (3) and (4), E_o* is the desired output voltage, r is the aggregate loss resistance and V_D is the forward voltage of the diode. T_S is the switching period and N_{Ts} are the resolution of digital PWM generator. r is omitted in (4) because it does not almost affect. Also, a and b are given by

$$a = A_{ei}G_{AD\_ei} \tag{5}$$

$$b = A_{eo}G_{AD\_eo} \tag{6}$$

Equations (3) and (4) are switched and applied depending on the operation modes of the dc-dc converter, which are the current continuous mode (CCM) and the current discontinuous mode (DCM). The model control can regulate e_o because the bias value is changed according to $i_{o\_nod}[n]$.

The digital value $T_{on\_PID}[n]$ is obtained by using $e_o[n\text{-}1]$ in the PID controller and its control equation is given by

$$T_{on\_PID}[n] = K_P\left(N_R - e_o[n-1]\right) + K_I\sum N_{I,n-1} + K_D N_{D,n-1} \tag{7}$$

where K_P, K_I and K_D are the proportional, integral and derivative coefficients, respectively. N_R is the reference value of the output voltage. $\Sigma K_{I,n}$ and $K_{D,n}$ are the result of calculation in the integral and the differential control at the n-th switching period.

$T_{on}[n]$ is determined by subtraction of $T_{on\_model}[n]$ and $T_{on\_PID}[n]$ as follows:

$$T_{on}[n] = T_{on\_model}[n] - T_{on\_PID}[n] \tag{8}$$

The DPWM generator outputs the PWM signal depending on $T_{on}[n]$ and the clock signal.

III. Output Current Prediction

In this section, the output current prediction is explained in detail. Its performance is confirmed in the simulation. $i_{o\_nod}[n]$ is predicted by using the $e_o[n\text{-}1]$ and $T_{on}[n\text{-}1]$ in the output current prediction part. The equations of the output current prediction are shown in

$$i_{o\_nod\_CCM}[n] = \frac{T_{on}[n](\frac{e_i[n-1]}{a} + V_D) - N_{Ts}(\frac{e_o[n-1]}{b} + V_D)}{rN_{Ts}} \tag{9}$$

$$i_{o\_nod\_DCM}[n] = \frac{(\frac{e_i[n-1]}{a} - \frac{e_o[n-1]}{b})(\frac{e_i[n-1]}{a} + V_D)T_s T_{on}^2[n-1]}{2L(\frac{e_o[n-1]}{b} + V_D)} \quad (10)$$

Figure 3 illustrates the characteristics of $i_{o\_nod}[n]$ against i_o. The gray solid line is the ideal value of $i_{o\_nod}[n]$. The one-dot chain line is calculated value using (9). The broken line is calculated value using (10). Equation (9) that predicts output current in CCM is larger than (10) in CCM. Likewise, Equation (10) that predicts output current in DCM is larger than (9) in DCM. Therefore, the switching of them is carried out by the comparison of (9) and (10). Considering the properties of (9) and (10), a larger one is applied as $i_{o\_nod}[n]$. In addition, the switching is seamless around the critical point and the calculated value is matched well with the ideal value.

Figure 4 shows the flow chart of the model control. Equations (9) and (10) are calculated simultaneously and compared with each other. A larger value of them is applied as $i_{o\_nod}[n]$ and the operation mode of the dc-dc converter is judged. $T_{on\_model}[n]$ is calculated according to the operation mode.

Figure 5 depicts the relationship of the ideal value of $T_{on}[n]$, (3) and (4) against i_o. The gray solid line is the ideal value of $T_{on}[n]$. The one-dot chain line is the calculated value using (3). The broken line is the calculated value using (4). As shown in Fig. 5, $T_{on}[n]$ is calculated ideally against i_o and the model equation is switched smoothly around the critical point. As a result, it is possible to perform the model control using $i_{o\_nod}[n]$.

A. Steady State

The static characteristics are shown in Fig. 6. The switching frequency f_S is 100 kHz. The circuit parameters are e_i = 20 V, E_o* = 5 V, L = 196 μH and C = 891 μF. The resolution of A-D converter is 11 bits and N_{TS} is 2000. K_P is 4, K_D is 4 and K_I is 0.00011. The upper and lower limit value N_{I_max} and N_{I_min} of the register for the integral value are set to 32000 and 32000, respectively. It is possible to regulate e_o from the light load to the heavy load.

B. Transient state

Figures 7 and 8 show the transient responses of the proposed method in the case of the load transient from DCM (R = 100 Ω) to CCM (R = 5 Ω), and vice versa. The proper damping ratio is set to suppress the oscillation of $i_{o\_nod}[n]$ in the transient state. Figures 7(a) and 8(a), the blue solid line is calculated value using (9). The red solid line is calculated value using (10). The black solid line is $i_{o\_nod}[n]$ used for model control. These figures show the switching of (9) and (10) and the output current prediction is operated in an appropriate manner. Also, Figs. 7(b) and 8(b) show the comparison of i_o and $i_{o\_nod}[n]$. The green solid line is the output current and the black solid line is $i_{o_nod}[n]$used for model control. As shown in Fig. 7(b), although $i_{o\_nod}[n]$ is off i_o at the beginning of the load transient, it converges proper value by reducing the oscillation of itself using damping ratio. On the other hand, it almost captures i_o in Fig. 8(b). Figs 7(c) and 8(c) depict the transient response of e_o. t_{cv} is the time when e_o converges within plus-minus 1% of E_o*. δ_{eo_under} and δ_{eo_over} are the undershoot and overshoot of e_o. In Fig. 7(c), δ_{eo_under} is 6.0% and t_{cv} is 5.7 ms. On the other hand, in 8(c), δ_{eo_over} is 4.2% and t_{cv} is 16.8 ms.

IV. Comparison of Transient Response

Figure 9 shows the transient responses of e_o in the case of the load transient from DCM to CCM, and vice versa. In this case, K_P is 4, K_D is 4 and K_I is 0.016. In Fig. 9(a), δ_{eo_under} is 9.3% and t_{cv} is 7.7 ms. δ_{eo_under} and t_{cv} of the propose method are improved by 35% and 26% compared with the conventional PID control. On the other hand, in Fig. 9(b), δ_{eo_over} is 4.2% and t_{cv} is 22.2ms. t_{cv} of the propose method is improved by 24% compared with the conventional PID control.

V. Conclusion

The current detection algorithm for sensorless model control dc-dc converter is presented in this paper. The switching of the predicted current is carried out smoothly around the critical point by the comparison of it. A larger value of the predicted output current is applied as the correct prediction value. The predicted value captures the ideal value in the static and transient state. As a result, the on-time of the switch is calculated with felicity. Therefore, the validity of the proposed method is demonstrated with simulation results. Moreover, the transient response of the proposed method is improved by at most 35%.

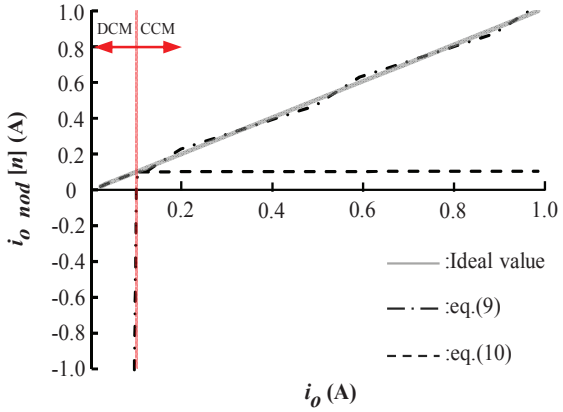

Fig. 3. Operation principle of predicted output current.

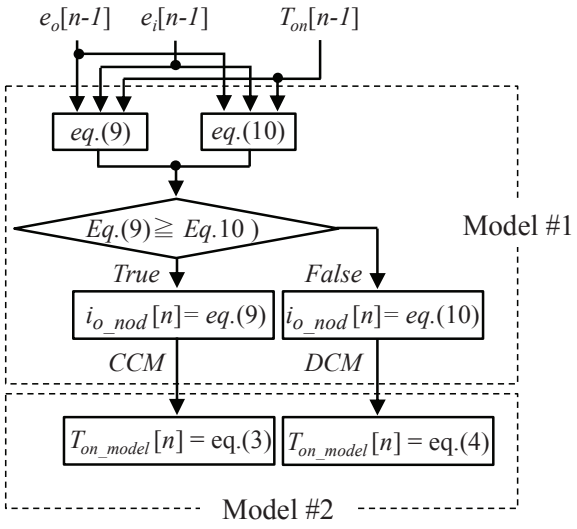

Fig. 4. Flow chart of model control.

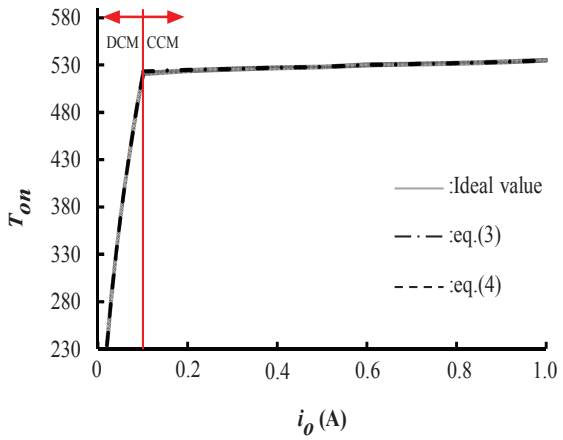

Fig. 5. Operation principle of on-time.

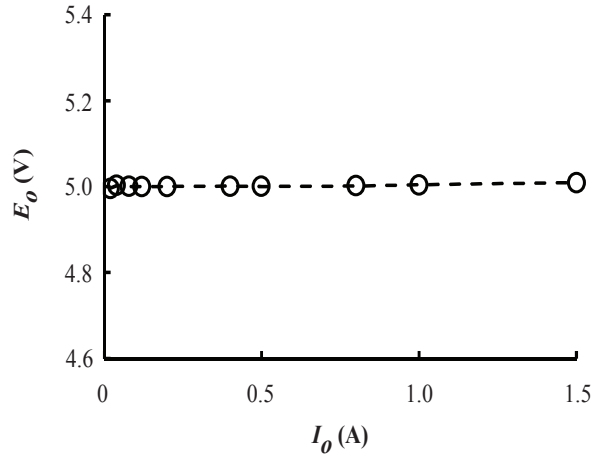

Fig. 6. Steady-state characteristics.

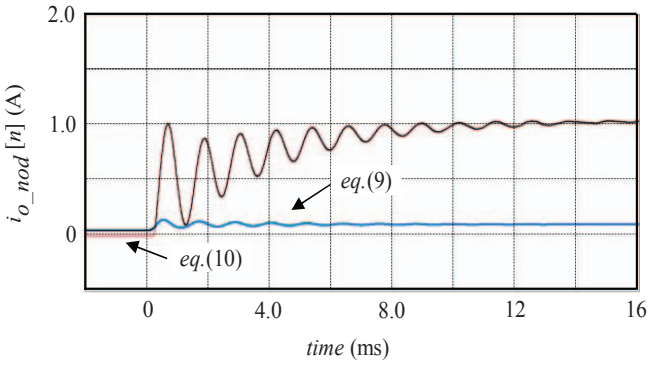

(a) Switching of predicted output current.

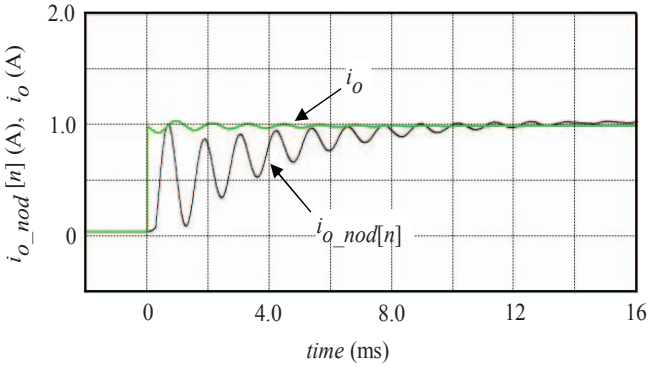

(b) Predicted output current against i_o

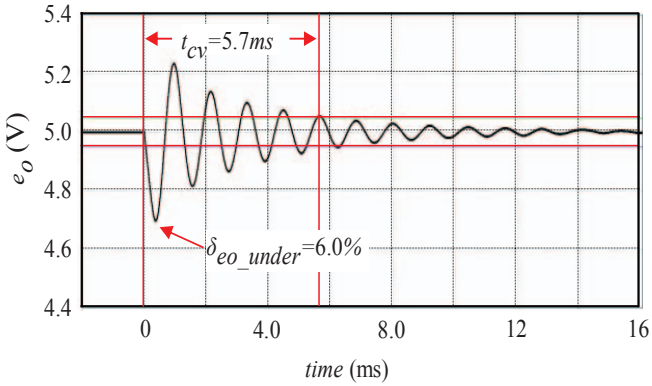

(c) Output voltage e_o.

Fig. 7. Transient response in proposed method.
(Load step from DCM to CCM.)

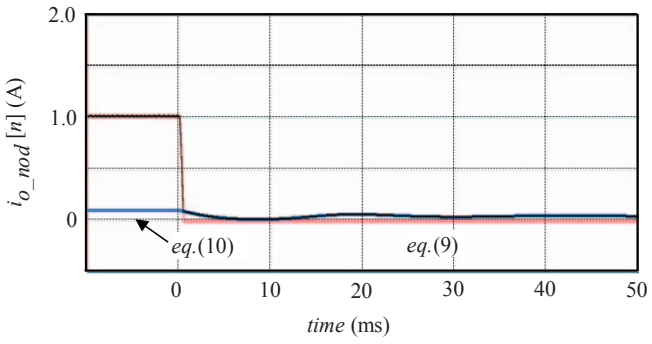

(a) Switching of the predicted output current.

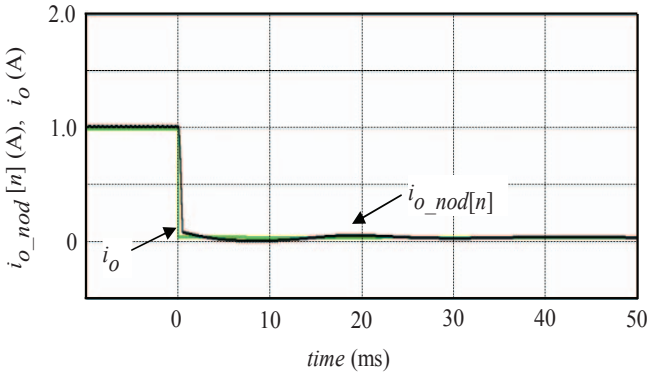

(b) Predicted output current against i_o.

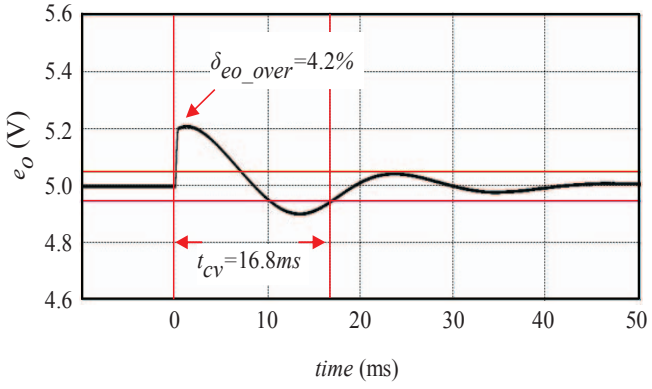

(c) Output voltage e_o.

Fig. 8. Transient response in proposed method.
(Load step from CCM to DCM.)

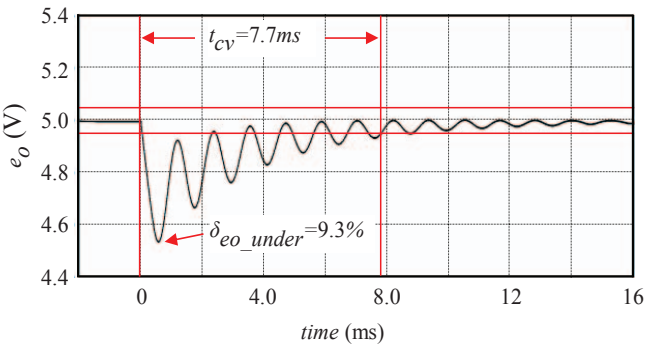

(a) Load step from DCM to CCM.

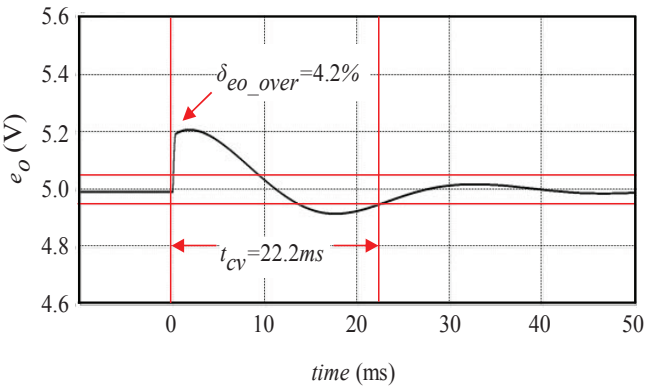

(b) Load step from CCM to DCM.

Fig. 9. Transient response in conventional PID control.

REFERENCES

[1] K. De Cuyper, M. Osee, F. Robert and P. Mathys, “A digital plat form for real-time simulation of power converters with high switching,” in Proc. IEEE Power Electronics and applications, pp. 1-10, Sept. 2011.

[2] R. C. N. Pilawa-Podgurski, W. Li, I. Celanovic and D. J. Perreault, “Integrated cmos dc-dc converter with digital maximum power point tracking for a portable thermophotovoltaic power generator,” Proc. of IEEE Energy Conversion Congress and Exposition, pp. 197-204, Sept. 2011.

[3] C. Wen, B. Fahimi, E. Cosoraba, Y. Fan, ” Stability analysis and voltage control method based on virtual resistor and proportional voltage feedback loop for cascaded dc-dc converters,” Proc. of Energy Conversion Congress and Exposition, pp. 3016-3022, Sep. 2014.

[4] F. Kurokawa, J. Sakemi, A. Yamanishi and H. Osuga, “A new quick transient response digital control dc-dc converter with smart bias function,” Proc. of International Telecommunications Energy Conference, pp. 1-7, Oct. 2011.

[5] D. Segaran, D. G. Holmes, B. P. McGrath, "Enhanced load step response for a bidirectional dc–dc converter," *IEEE Trans. Power Electronics*, Vol. 28, No.1, pp. 371-379, Jan., 2013.

[6] F. Kurokawa and S. Hirotaki, “A new high performance dc-dc converter with sensorless model reference modification,” in Proc. IEEE Telecommunications Energy Conference , pp1-5, Sep. 2014.

[7] F. Kurokawa and S. Hirotaki, “A novel sensorless model control dc-dc converter,” in Proc. IEEE Renewable Energy Research and Application , pp 663 - 667, Oct. 2014.

[8] F. Kurokawa and S.Hirotaki, “Model control dc-dc converter without current detection,” in Proc. IEEE International Conference on Intelligent Green Building and Smart Grid, pp. 1-5, Apr. 2014.